Mobile ground-based measurements of aerosol and trace gases during a prescribed burning experiment in boreal forest in Finland

Liisa Pirjola[1)2)]*, Aki Virkkula[2], Tuukka Petäjä[2], Janne Levula[3], Jaakko Kukkonen[4] and Markku Kulmala[2]

[1)] *Department of Technology, Metropolia University of Applied Sciences, FI-00180 Helsinki, Finland (*corresponding author's e-mails: liisa.pirjola@metropolia.fi, or liisa.pirjola@helsinki.fi)*
[2)] *Department of Physics, FI-00140 University of Helsinki, Finland*
[3)] *Hyytiälä Forestry Field Station, University of Helsinki, FI-35500 Korkeakoski, Finland*
[4)] *Finnish Meteorological Institute, Atmospheric Composition, FI-00101 Helsinki, Finland*

As a part of the EUCAARI and IS4FIRES projects, a prescribed burning experiment was conducted near the SMEAR II station in Hyytiälä, Finland, on 26 June 2009. The ground-level concentrations of the smoke at different distances from the burn area were measured by a mobile laboratory van "Sniffer". The maximum of the total particle number concentration, N_{tot}, was 2.7×10^6 cm^{-3} at a distance of around 180 m from the burn area. The number size distribution had two modes peaking at 12–16 nm and 90–100 nm during the flaming phase, and three modes peaking at 6–10 nm, 42–70 nm, and 260–460 nm during the smouldering phase. The accumulation and coarse mode particles dominated the volume size distributions. The emission ratios were calculated for N_{tot}, PM$_{2.5}$, CO and NO$_x$ in regard to the excess CO$_2$ concentration. The obtained emission factors EF (number or mass per kg fuel burned) were 18.4×10^{15} kg^{-1}, 29.0 g kg^{-1}, 52.1 g kg^{-1}, and 2.7 g kg^{-1} for N_{tot}, PM$_{2.5}$, CO and NO$_x$, respectively.

Introduction

Biomass burning strongly affects environment and climate, since it is the largest global source of trace gases and aerosol particles (e.g. Crutzen and Andreae 1990). Emitted gases, such as carbon monoxide (CO), nitrogen monoxide (NO), sulphur dioxide and hydrocarbons influence global tropospheric chemistry (e.g. Andreae and Merlet 2001, Hobbs *et al.* 2003), because, e.g., chemical reactions of NO and organics along with photo- chemistry lead to the formation of ozone. Ozone, in turn, is a greenhouse gas and an important atmospheric oxidant as well as a precursor of OH radicals (e.g. Hobbs *et al.* 2003, Fiedler *et al.* 2010). Aerosol particles play an important role in the Earth's radiation balance directly by scattering solar radiation back to space and indirectly by providing a source of cloud condensation nuclei (CCN) (e.g. Crutzen and Andreae 1990, Charlson *et al.* 1992, Hobbs *et al.* 2003, Sinha *et al.* 2003, Bond *et al.* 2013). Long-range transport of bio-

---

mass plumes is an important factor to control the spatial and temporal variability of aerosol properties and atmospheric particle load.

In the measurements of Reid *et al.* (2005), fresh smoke particles were composed of ~50%–60% organic carbon and ~5%–10% black carbon, with count median diameters in the range of 100–160 nm peaking at ~130 nm. Regarding boreal forest fires, Saarnio *et al.* (2010) showed that most of the sub-micrometer particulate mass was organic matter. Petzold *et al.* (2007) studied the plumes from large wildfires in North America, which were transported to central Europe at 3–8 km altitude in 10 days. Furthermore, Fiedler *et al.* (2010) predicted that during transport across the Atlantic, the aged African smoke particles have a potential to become activated already at very small supersaturation (0.05%), which would allow them to act as CCNs in maritime stratiform cloud formation. Hodzic *et al.* (2007) showed that the presence of elevated smoke layers over Europe significantly altered atmospheric radiative properties. Their model results imply a 10% to 30% decrease in photolysis rates and an increase in atmospheric radiative forcing of 10–35 W m^{-2} during the period of strong fire influence throughout a large part of Europe.

Biomass burning contributes significantly to the air quality at regional and local scales, especially by increasing particle concentrations and causing harmful health effects. Pollution episodes associated with wildfire emissions have been observed worldwide (Kumar *et al.* 2013). Sofiev *et al.* (2007) and Saarikoski *et al.* (2007) showed that wildfire plumes originated in Russia and central-eastern Europe can also substantially affect central and western Europe, and the Nordic countries. In some cases, wildland fire plumes may occur simultaneously with anthropogenic air pollution and substantial concentrations of allergenic pollen (Klein *et al.* 2012). Forest wildfires have been on the rise in recent decades. Westerling *et al.* (2006) reported temporally increasing large-wildfire frequency, longer wildfire durations, and longer wildfire seasons in the western USA. This trend might result in the situation that forests will become a source of increased atmospheric CO$_2$ rather than a sink; furthermore, this will be promoted by increased temperature and reduced precipitation.

Other reasons for increasing wildfires might be changes in farming and land use (Carvalho *et al.* 2010).

Recently, numerous studies including laboratory burns, *in situ* experiments, remote sensing, and modelling have been published; these have been reviewed by Andreae and Merlet (2001), Reid *et al.* (2005), Kumar *et al.* (2012) and Agaki *et al.* (2011). Emission factors, i.e., mass of any compound emitted per burned biomass, are relatively well known for grass and bush fires; however, large uncertainties still exist regarding emission factors of boreal, temperate and some tropical forests (Reid *et al.* 2005, Janhäll *et al.* 2010). Average emission factors are not sufficient for plume dispersion modelling, since smoke properties vary as a function of fuel type and moisture, combustion phase (ignition, flaming and smouldering), and meteorological conditions (Reid *et al.* 2005). In flaming combustion (when the burning temperature is relatively high), particle formation begins with the creation of condensation nuclei, such as PAH from ejected fuel gases as well as from a variety of soot-like species (Reid *et al.* 2005), onto which condensable vapours can condensate. In smouldering combustion (lower burning temperature), the mass fraction of soot in smoke particles is very low, and particles are largely formed by the condensation of volatilized organics on any available particles or surfaces (Reid *et al.* 2005, Maruf Hossain *et al.* 2012).

On 26 June 2009, a prescribed burning experiment was conducted near the SMEAR II station in Hyytiälä, southern Finland, as part of the EUCAARI (European Integrated Project on Aerosol Cloud Climate Air Quality Interactions) and the IS4FIRES (Integrated Monitoring and Modelling System for Wildland Fires) projects. The aim of the prescribed burning was to burn the logging waste, surface vegetation and the uppermost part of the raw humus layer in the second summer after the clear cut of the forest. This practise, which is common in southern Finland, promotes regeneration of a tree stand and is followed by planting Scots pine and occasionally silver birch. The general goal of the campaign was to provide comprehensive data for estimating the effect of forest fires on air quality and climate. More specific goals were to study aero-

sol chemical composition and physical characteristics, concentrations of gaseous compounds, smoke dispersion both horizontally and vertically, detection of fires using satellite remote sensing, and modelling both the spreading and heat production of the fire, and atmospheric dispersion of the fire plume. The overview of the campaign is described in Virkkula *et al.* (2014b), and the results from the aircraft measurements are described in Virkkula *et al.* (2014a). Kukkonen *et al.* (2014) evaluated the atmospheric dispersion of plumes from this prescribed burning campaign using a plume rise model, and compared the model predictions with particulate matter number concentration measurements from an aircraft.

Our objective was to study (1) ground-level dispersion of particles and trace gases of the smoke plume, and (2) aerosol physical characteristics, as well as (3) to derive the emission parameters representing the prescribed burning of logging slash in a boreal forest. The measurements were performed using a research van called "Sniffer". Such special mobile research van techniques have not previously been applied for studying the dispersion and properties of plumes from prescribed fires.

Methods

Fire characteristics

The size of the burning area was approximately 0.8 ha and it was located near the SMEAR II forest field station (61°50´50.685´´N, 24°17´41.206´´E, 179 m a.s.l.) in Hyytiälä, southern Finland (Hari and Kulmala 2005), 300–500 m southwest from the SMEAR II measurement buildings and the measurement mast (Fig. 1). The burning started on 26 June 2009 at 07:45 local winter time (EET, UTC + 2). We use the local winter time throughout this paper. Since the more detailed description of the burning can be found by Virkkula *et al.* (2014b), fire characteristics are only briefly discussed below.

In February 2009, all trees — aged of around 50 years — were cut, but some tree trunks, all tree tops and all branches as well as surface vegetation, litter-layer and uppermost part of the
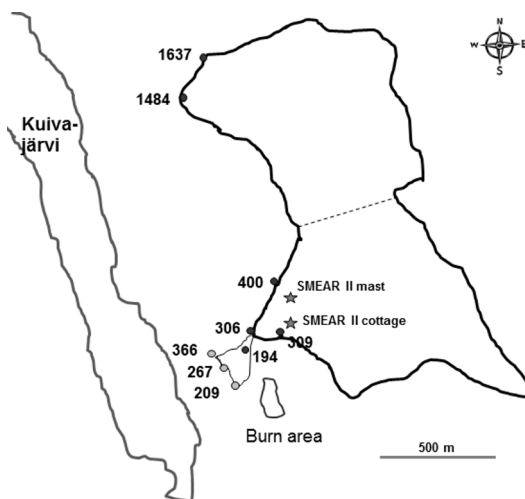

Fig. 1. The burn area and the measurement setup in Hyytiälä, Finland. Mobile measurements by "Sniffer" were performed along the 5.8-km-long circular road (black line). The dots indicate the sites, where "Sniffer" was stopped for stationary measurements during the flaming (black dots) and smouldering (gray dots) phases. The numbers indicate the distances in meters from the centre of the burn area.

humus-layer were left on the ground. The area composed of 64% of slash, 4% of surface vegetation and 32% of humus-layer. The total mass of the organic material burned was estimated to be 46.8 tonnes. The prescribed burning was performed as described in Virkkula *et al.* (2014b). Burning, including both the flaming and smouldering phases lasted from 07:45 to 13:00 EET. The flaming phase (active burning) was visually over at 10:00 EET. The accurate durations of flaming and smouldering periods could not be determined accurately. Yokelson *et al.* (1996) found in their laboratory studies that the modified combustion efficiency (MCE) is around 0.99 for pure flaming and around 0.8 for pure smouldering. In our case, the MCE was always greater than 0.94, and no clear difference was observed during the flaming and smouldering phases. On the other hand, the response time of our CO analyser was more than 30 s and the values were running averages; the peak concentration values that correspond to smaller time averages evidently could be higher.

On 26 June 2009, the weather was warm and sunny, the temperature varied from 20 °C in the morning to 26 °C at noon, and the rela-

tive humidity ranged from 55% to 30%. The wind speed at 34 m altitude was rather constant and low, around 1–2 m s^{-1}, during the first two burning hours, but later varied from 1 to 5 m s^{-1}. At the start of the burning, the wind blew from the southwest (~240° measured at 35 m altitude), but soon turned to blow from the south and later from the southeast (~120°). Therefore, the SMEAR II station was not able to detect the most intensive smoke plume (Virkkula *et al.* 2014b). The inverse Monin-Obukhov length, L^{-1} = –0.0012 m^{-1} at 14:00 EET, evaluated by Kukkonen *et al.* (2014) indicated a moderately unstable condition. The prevailing meteorological conditions resulted in an upright plume during the flaming stage that ascended to fairly high altitudes, according to both measurements and modelling (Kukkonen *et al.* 2014). Consequently, only a small fraction of the plume dispersed near the ground during the flaming phase, contrary to the beginning of the smouldering phase when no flames were visible but dense smoke dispersed close to the ground surface.

Mobile measurements and instrumentation

Ground-level concentrations and dispersion of the smoke plume near the ground were measured by a research laboratory van named "Sniffer" (Volkswagen LT35 diesel van) (Pirjola *et al.* 2004, 2006, 2012). The van was driven in the forest along the only possible road nearby the burning area with the speed of 15–20 km h^{-1} (Fig. 1). The length of this narrow route was 5.8 km, and it was driven twice during the campaign. Additionally, "Sniffer" was parked at road sides at the distances of 200–1600 m from the burning area (Fig. 1) for 10 minutes to monitor the plume during the times when some smoke visually seemed to descend. Sampling was performed at the altitude of 2.4 m from the ground, above the van's windshield. Furthermore, students were walking in the forest along three ring footpaths at the distances of around 1500–1600 m, 1000–1100 m and 100–200 m from the burning area, carrying three GPS receivers and portable particle counters CPC 3010 (TSI, Inc.). The dilution ratio for the CPCs was 3.1.

Particle number concentration and size distribution were measured by an Electrical Low Pressure Impactor (ELPI, Dekati Ltd.) with the flow rate of 10 lpm (Keskinen *et al.* 1992) equipped with a filter stage (Marjamäki *et al.* 2002) and an additional stage designed to enhance the particle size resolution for nanoparticles (Yli-Ojanperä *et al.* 2010). ELPI classified particles in the size range of 7 nm–10 μm (aerodynamic diameter) to 12 classes with 1-s time resolution. The cut-off diameters of the ELPI stages were 0.016 (additional stage), 0.030, 0.056, 0.093, 0.156, 0.264, 0.385, 0.617, 0.954, 1.610, 2.410, and 9.97 μm. The total particle concentration (10 nm–1 μm) was also monitored by a condensation particle counter CPC 3010 (TSI, Inc.) through a passive clean air dilution system with a dilution ratio of 5:1.

A DustTrak (TSI, model 8530) with a 2.5 μm inlet was used to measure the real-time PM$_{2.5}$ concentrations (i.e. particles < 2.5 μm in aerodynamic diameter) with a time resolution of 1 s. The DustTrak operates based on a light scattering technique where the amount of the scattered light is proportional to the volume concentration of the aerosol. The instrument was factory calibrated with Arizona dust particles, and it has been shown to overestimate ambient particle mass concentrations (e.g. Morawska *et al.* 2003, Kingham *et al.* 2006). Because no simultaneous gravimetric measurements of PM$_{2.5}$ were performed, we inferred PM$_{2.5}$ also from the ELPI data. The smoke particles were assumed to be spherical with the density of 1.3 g m^{-3}. Reid *et al.* (2003) report that besides organic material, typically 15% of fresh smoke particle mass is either black carbon or trace inorganic species, and therefore the average density of dry smoke particles likely varies in the 1.2–1.4 g cm^{-3} range. The ELPI PM$_{2.5}$ mass concentrations were 35.4% of the DustTrak PM$_{2.5}$ mass concentrations with the correlation coefficient of 0.97. Therefore, all DustTrak PM$_{2.5}$ data were divided by a factor of 2.83. This factor is close to the one suggested by Morawska *et al.* (2003).

Also monitored by "Sniffer" with 1 s time resolution were gaseous concentrations such as carbon monoxide CO (Model CO12M, Environnement S.A.), nitrogen oxides NO, NO$_2$ and NO$_x$ (Model APNA 360, Horiba) as well as

carbon dioxide CO_2 (Model VA 3100, Horiba). An ultrasonic wind sensor (Model WAS425AH, Vaisala) on the roof of the van at 2.9 m height provided the relative wind speed and direction. Temperature and relative humidity were recorded by the humidity and temperature probes (Model HMP45A, Vaisala). A global position system GPS (model GPS V, Garmin) saved the van's speed and the driving route.

All instruments were synchronized before the start of the measurements. For all the data, the 10-s averages were calculated to reduce the noise in the instruments.

Emission parameters

Emission ratios (ER) and emission factors (EF) of particulate and gaseous species are useful parameters in describing emissions during the burning. Emission ratio ER_X is defined as the excess molar ratio of species X divided by the excess molar ratio of a reference gas such as CO_2 or CO (e.g. Andreae and Merlet 2001, Sinha *et al.* 2003, Guyon *et al.* 2005). Emission ratio can be written as

$$ER_x = \frac{X - X_{bg}}{CO_2 - CO_{2,bg}} = \frac{\Delta X}{\Delta CO_2}, \qquad (1)$$

where X and X_{bg} refer to the species and the ambient background concentrations, respectively. In this work, we inferred ER_X directly from the regression slope of the concentration of ΔX *versus* ΔCO_2 (Yokelson *et al.* 2007), when X is CO, NO, NO_x, $PM_{2.5}$ or N_{tot} (> 7 nm) concentration.

Combustion efficiency (CE) is the amount of carbon released as CO_2 from a fire to the total excess carbon emitted (Ward and Hardy 1991). The carbon can be emitted as CO_2, CO, CH_4, non-methane organic carbon (NMHC) and particulate organic carbon (POC). However, Hobbs *et al.* (2003) showed that the emission of CO is closely linked to the emission of CH_4, NMHC and POC. The modified combustion efficiency (MCE) can be evaluated as follows:

$$MCE = \frac{\Delta CO_2}{\Delta CO_2 + \Delta CO}. \qquad (2)$$

The difference between CE and MCE is typically only a few percent (Hobbs *et al.* 2003). The

ER_{CO} and MCE describe the relative amount of flaming and smouldering combustion for biomass burning; higher ER_{CO} and consequently lower MCE indicates more smouldering (Yokelson *et al.* 2007).

Finally, the emission factor EF_X (g kg^{-1} fuel burned) is the amount of a compound X released per amount of dry fuel consumed. In this work, we utilised the molar emission ratios and use the formula presented by Andreae and Merlet (2001):

$$EF_x = ER_x \frac{M_x}{M_{CO_2}} EF_{CO_2}, \qquad (3)$$

where M_X and M_{CO2} are the molar masses of the species X and CO_2, and EF_{CO2} is the emission factor of the reference species CO_2. Based on airborne measurements from five Canadian boreal forest fire plumes Simpson *et al.* (2011) reported an average EF_{CO2} of 1616 ± 180 g kg^{-1}, whereas Urbanski *et al.* (2013) slightly smaller value of 1596 ± 23 g kg^{-1} from wildfire-season fires in mixed conifer forests in the USA, and Burling *et al.* (2011) somewhat higher value of 1668 ± 72 g kg^{-1} from conifer forest understory burns in the USA. For this work, we adopted the value from Simpson *et al.* (2011).

Results and discussion

Temporal variation of the concentrations

Before the fire was ignited, "Sniffer" was driven counterclockwise along the route (Fig. 1). These measurements provided the background concentrations at 07:03–07:28 EET. The average particle number concentration was 2710 cm^{-3}, indicating clean air. The average background concentrations of CO and CO_2 were 130 ppb and 395 ppm, respectively. The NO and NO_x background concentrations were below the detection limit of the NO_x analyser (50 ppb) and thus set to 0 ppb (Table 1). The corresponding background concentration values, measured at the SMEAR II mast for gases at the altitude of 4.2 m, and at the aerosol cottage for particles (Fig. 1), are also given in Table 1.

During the flaming stage, "Sniffer" ran the route at 08:44–09:25 EET; however, at this time it was stopped for around 10 minutes at differ-

ent sites in the range of 200–1600 m from the centre of the burning area (Fig. 1). Due to the meteorological conditions, especially the low wind speed and the substantial buoyancy of the plume as explained above, most of the smoke ascended steeply during the flaming period; only a small fraction of the plume dispersed near the ground level. Relatively higher particle concentrations were measured along the western part of the route. During the smouldering period, starting at 10:00 EET, a dense smoke dispersed at lower altitudes. It was therefore feasible to use "Sniffer" to monitor the plume closer to the centre of the burn area, at the distances of around 200–400 m (Fig. 1).

When exploring the time evolution of particle number size distribution measured by ELPI (Fig. 2a), we found that the accumulation mode particles were always present, peaking roughly at 100–150 nm, whereas the nucleation mode particles appeared only if the smoke was visually found to be dispersed at the monitor height. During the smouldering phase, the particle concentrations were higher and the bursts continued for a longer time than during the flaming phase (Fig. 2b). The highest particle number concentration at a distance of ~180 m from the centre of the burning area was 5.6×10^5 cm^{-3} during the flaming phase, and 2.7×10^6 cm^{-3} during the smouldering period. Similar concentrations at the corresponding distances from the source area were also reported by Virkkula *et al.* (2014a)

Table 1. Background concentrations ± SD before the start of the prescribed burning, measured at the mobile van Sniffer, at the stationary SMEAR II mast and at the aerosol cottage.

Background concentrations	Sniffer (2.4 m above ground level)	SMEAR II
N_{tot} (cm^{-3})	2713 ± 270	2265 ± 120[b]
PM$_{2.5}$ (μg m^{-3})	8.9 ± 1.0	–
CO (ppb)	126 ± 36	122 ± 3[c]
CO$_2$ (ppm)	395 ± 6	416 ± 5[c]
NO (ppb)	0[a]	0.39 ± 0.37[c]
NO$_x$ (ppb)	0[a]	0.39 ± 0.11[c]

[a] below the detection limit of the instrument.
[b] SMEAR II aerosol cottage, inlet at about 5 m above ground level.
[c] SMEAR II mast at 4.2 m above ground level.

based on the airborne measurements. The total number concentrations measured by the CPC and the ELPI were in good agreement with each other during the flaming phase (Fig. 2b), although the instruments had slightly different cut-off sizes for particles: 10 nm for CPC and 7 nm for ELPI. However, during the smouldering phase, CPC was not able to record the highest concentrations since it became saturated at the concentration of ~3×10^5 cm^{-3}.

As expected, the peak values of the PM$_{2.5}$ concentrations (Fig. 2c) occurred simultaneously with the peaks of the number concentrations. During the smouldering phase the highest peak concentrations were almost three orders of magnitude higher than the average background concentration.

Similarly, the elevated CO$_2$ concentrations coincided with the peak concentrations of particle numbers and masses (Fig. 2d). The highest CO$_2$ concentrations, approximately 80–100 ppm above the background concentration, were measured during the smouldering phase. We selected the distinct CO$_2$ peak values (circles in Fig. 2d) along with the corresponding particle and other gas concentrations for a more detailed analysis. The emission parameters were inferred based on these selected maximum values.

Spatial variation of the concentrations

The horizontal dispersion of the smoke plume at the ground level was also measured by the pedestrians walking along three routes at three distances from the burning area. Large variation in the particle number concentrations was observed (Fig. 3); the highest value (3.1×10^5 cm^{-3}) was detected on the closest route at around 170 m distance from the burn are. On the next closest route, the highest concentration was 5.3×10^4 cm^{-3} and on the farthest 1.4×10^4 cm^{-3}. These values were not detected simultaneously.

The peak values (calculated as 10-s averages from 1-s ELPI data) of the particle number concentrations corresponding to the CO$_2$ peaks (Fig. 2d) were calculated as a function of the downwind distance from the centre of the fire area (Fig. 4). To complement the "Sniffer" measurements, included were some points of the CPC
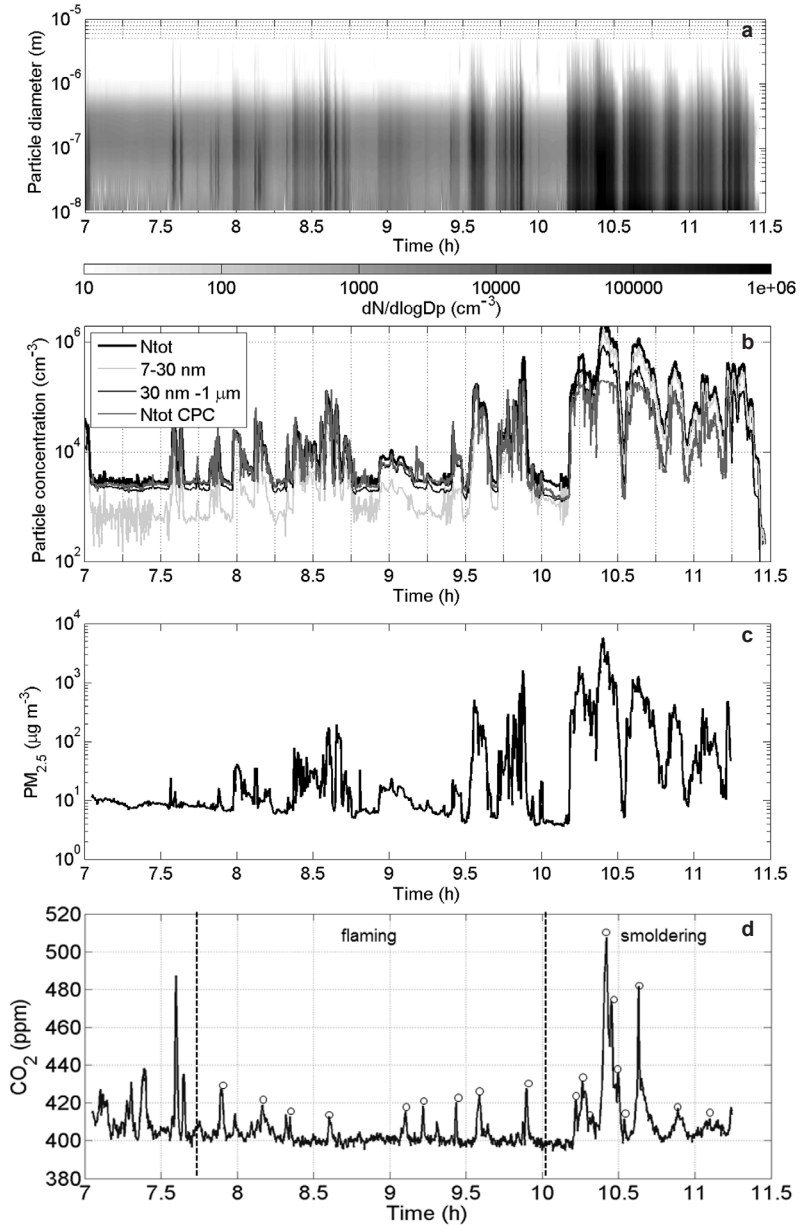
Fig. 2. (**a**) Time evolution of particle number size distribution, (**b**) total particle number concentration measured by ELPI (N_{tot}) and CPC (N_{tot} CPC), as well as concentrations of particles < 30 nm (7–30 nm) and ≥ 30 nm (30 nm–1 μm), (**c**) $PM_{2.5}$, and (**d**) CO_2. The concentrations were measured by the instruments on board the "Sniffer" van. The data corresponds to the values measured along the driving route.

data measured by the walking students (marked as "flaming CPC" in the legend to Fig. 4). As expected, the concentrations decreased as the distance increased, but still at a distance of 1.6 km from the centre of the burning area the concentrations were notably higher than the background value. The concentrations were two or three orders of magnitude higher during the smouldering phase as compared with those in the flaming phase.

Measurements of particle number concentrations at various distances from a single source are very scarce in the literature. However, such measurements could be used in the testing and evaluation of combined dispersion and aerosol process modelling. We therefore fitted a simple power function to the measured particle number concentrations in the flaming phase, N_{tot} (cm^{-3}) = $9.64 \times 10^6 d^{-1.01}$, where d is the distance in metres. Virkkula *et al.* (2014b) presented a slightly dif-
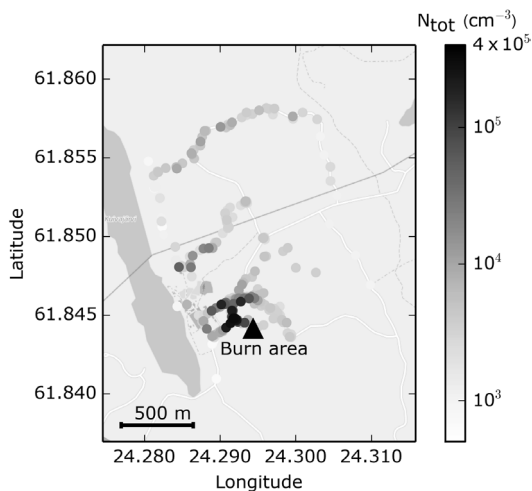
Fig. 3. Particle number concentrations (N_{tot}) of the smoke plume at the ground level as measured by portable CPCs carried by the walking researchers. The centre of the burn area is marked with a black triangle.

Fig. 4. The peaks of the total particle number concentrations as a function of downwind distance, *d* (m), from the centre of the burning area (10-s averages). Average background concentration was ~2700 cm^{-3}, shown as the horizontal dotted line. The curve was fitted to the measurements in the flaming stage using the equation N_{tot} (cm^{-3}) = 9.64 × 10$^6 d^{-1.01}$ (r^2 = 0.47, *p* = 0.0014). Measurements by "Sniffer" (ELPI) and the walking researchers (CPC) are presented.

ferent power function based on the "Sniffer" data but that data were collected during the smouldering phase. At 10:20–10:50 EET, "Sniffer" was standing for 5–10 minutes at three sites, which were at the distances of 209, 267 and 366 m downwind from the centre of the fire area (Fig. 1). The topography and the buildings prevented measurements from farther afield.

Dispersion of the gases and particles of the smoke plume during the smouldering phase were investigated by calculating the mean values of the top quartiles (the highest 25% of the data) for the measurement periods. The background concentrations were subtracted. As expected, the emitted concentrations decreased as the distance increased: from 101 ppm to 21 ppm, 3.5 ppm to 0.3 ppm, 2.3 × 10^6 cm^{-3} to 8.4 × 10^5 cm^{-3}, and 4.6 g m^{-3} to 0.8 g m^{-3} for CO_2, CO, N_{tot} and $PM_{2.5}$, respectively (Fig. 5). An exception was NO_x, but even then the mean concentrations measured from a stationary van decreased; 107 ± 48, 87 ± 62, 32 ± 37 ppb at distances 209, 267 and 366 m, respectively.

Spatial variation of particle size distributions
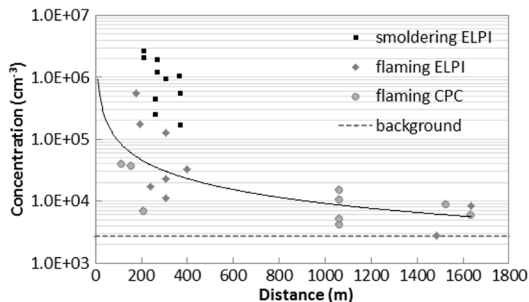
The particle size distributions were calculated

for the mean values of the top quartiles, i.e., the highest 25% of the data, for the times when the "Sniffer" van was stationary (around 10 minutes between 9:00–10:00 EET) at different distances from the burn area.

During the flaming phase, there were two modes in the particle number size distributions; the nucleation modes peaked at 11–16 nm and the accumulation modes at 90–101 nm (Fig. 6a). At the distance of 1484 m, no notable smoke was transported to "Sniffer", and the size distribution almost overlapped that of the background particles. The averaged background size distributions were measured just before the burning started, by both ELPI in "Sniffer" and the ground-level DMPS (Differential Mobility Particle Sizer) at the SMEAR II cottage (Fig. 1). Although the DMPS used mobility diameter and ELPI aerodynamic diameter when classifying particles, the size distributions were merged for particles > 40 nm. However, ELPI overestimated the concentration of the smallest particles.

After subtracting the background concentration (Fig. 6b), the lognormal parameters (number concentration, geometric mean diameter D_g and geometric standard deviation) were fitted into the modes of the number size distributions (Table 2). Two features can be noted. First, the closer to the burning area "Sniffer" was standing, the more particles in the nucleation and in

Fig. 5. Concentrations and standard deviations for the upper quartile of the data (the highest 25% of measured values) for N_{tot} (cm^{-3}), PM$_{2.5}$ (μg m^{-3}), NO$_x$ (ppb), CO$_2$ (ppm), and CO (ppm) for the measurement periods as a function of distance from the centre of the fire area during the smouldering phase. Background concentrations (Table 1) were subtracted
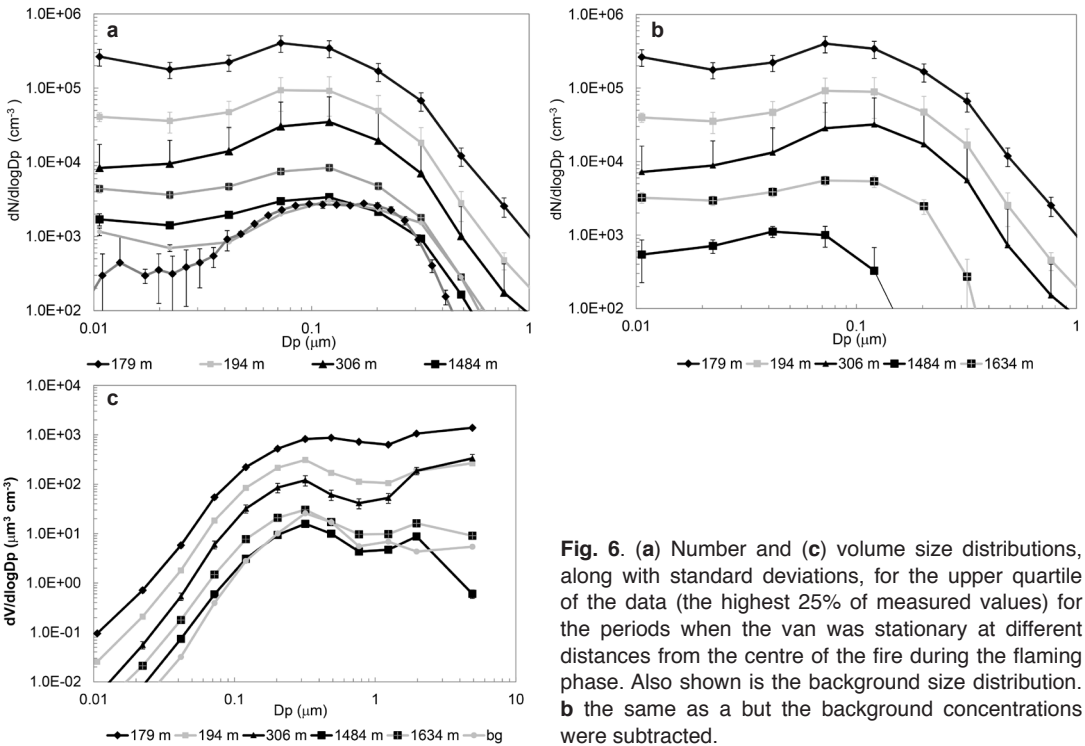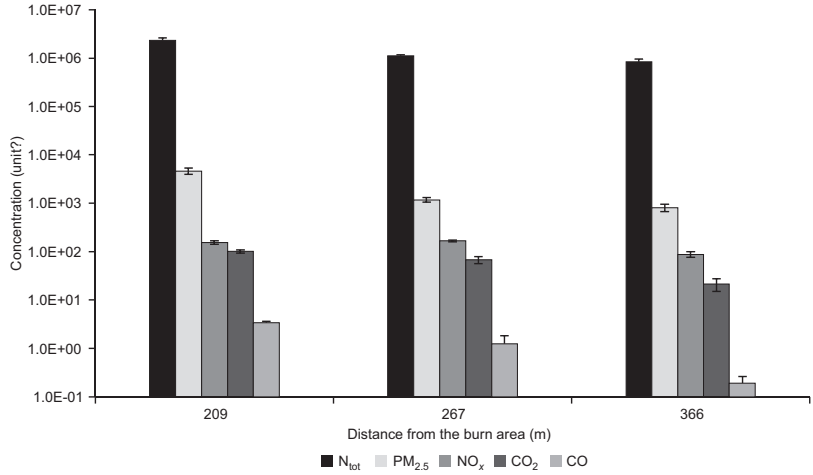

Fig. 6. (**a**) Number and (**c**) volume size distributions, along with standard deviations, for the upper quartile of the data (the highest 25% of measured values) for the periods when the van was stationary at different distances from the centre of the fire during the flaming phase. Also shown is the background size distribution. **b** the same as a but the background concentrations were subtracted.

the accumulation mode were observed. Second, for both modes, the diameter (D_g) increased with an increasing distance, indicating that during dispersion the particles had probably grown larger. Since the wind speed near the ground level was 1–2 m s^{-1}, the time of the plume to be transported to "Sniffer" standing at a distance of 1634 m was in the range of around 14–27 min. This time is sufficient for the particles to grow as a result of

condensation and coagulation processes (Seinfeld and Pandis 1998). The volume size distributions showed 2–3 modes which peaked at 28–38 nm, 100–200 nm and 1.4–1.9 μm (Fig. 6c). The accumulation and coarse mode particles played a major role closer to the burning area. These results are qualified since the size distributions at different distances were not measured simultaneously, and they significantly depended on the

temporal evolution of the prescribed fire and on the dispersion of the fire plume.

During the smouldering phase, both the number and volume concentrations in the size distributions in the smoke were from two to three orders of magnitude higher than those of the background air particles (Fig. 7). Although both the intensity of the fire and the dispersion conditions continuously varied in time, the standard deviations of the highest 25% concentration values were fairly small. The number size distributions (Fig. 7a) possessed three modes: the nucleation mode peaked at 6–10 nm, the Aitken mode at 42–70 nm, and the accumulation mode at 260–460 nm (Table 2). During atmospheric transport, the concentrations naturally decreased, but since the modal diameters increased, aerosol dynamics might play some role as well. The volume size distributions (Fig. 7b) consisted of four modes; the nucleation, Aitken, accumulation and coarse modes, the last of which dominated. The modes peaked at 15–30 nm, 59–65 nm, 300–400 nm, 1.7–3 μm, respectively.

Two main differences regarding the particle size distributions during the flaming and smouldering phases can be emphasized. First, the particle number concentration during the smouldering phase was around 10 times higher as compared with that during the flaming phase. In the flaming stage, the Aitken mode particles were typically dominant contrary to the smouldering phase, in which the nucleation mode particles

dominated. Airborne measurements by Virkkula *et al.* (2014a) also showed that in the smouldering phase new particles were able to be formed.

Second, the nucleation mode particles were smaller in the smouldering phase, and the accumulation mode particles, observed in the flaming phase, were shifted to the smaller Aitken mode sizes in the smouldering combustion. Likewise, the size segregated particle number emission factors increased further above that for the flaming phase (Fig. 7c) as also found by Hobbs *et al.* (1996). A reason might be a different combustion process, since the fire temperature was lower in the smouldering phase. Although the accumulation mode number concentrations during smouldering were less than 2% of the total concentrations (Table 2), they strongly affected the volume size distributions. Because the results presented in this work were monitored at 09:00–10:00 EET and at that time SMEAR II did not catch the smoke plume, the size distribution trends cannot be compared with those presented in Virkkula *et al.* (2014b).

Maruf Hossain *et al.* (2012) studied particle number emissions at 20 nm–10 μm range from oak and pine combustion, and found two modes, which peaked at around 150 nm and 500–600 nm, in both flaming and smouldering combustion conditions. Contrary to the smouldering condition, the flaming condition resulted in higher particle numbers in the smaller mode and lower particle number in the larger mode.

Table 2. Lognormal parameters for the fitted modes when the background particles were subtracted. N_{nuc}, N_{ait} and N_{acc} (cm^{-3}) refer to the particle number concentrations in the nucleation, Aitken and accumulation modes, respectively, D_g (nm) is the geometric mean diameter, and σ the geometric standard deviation.

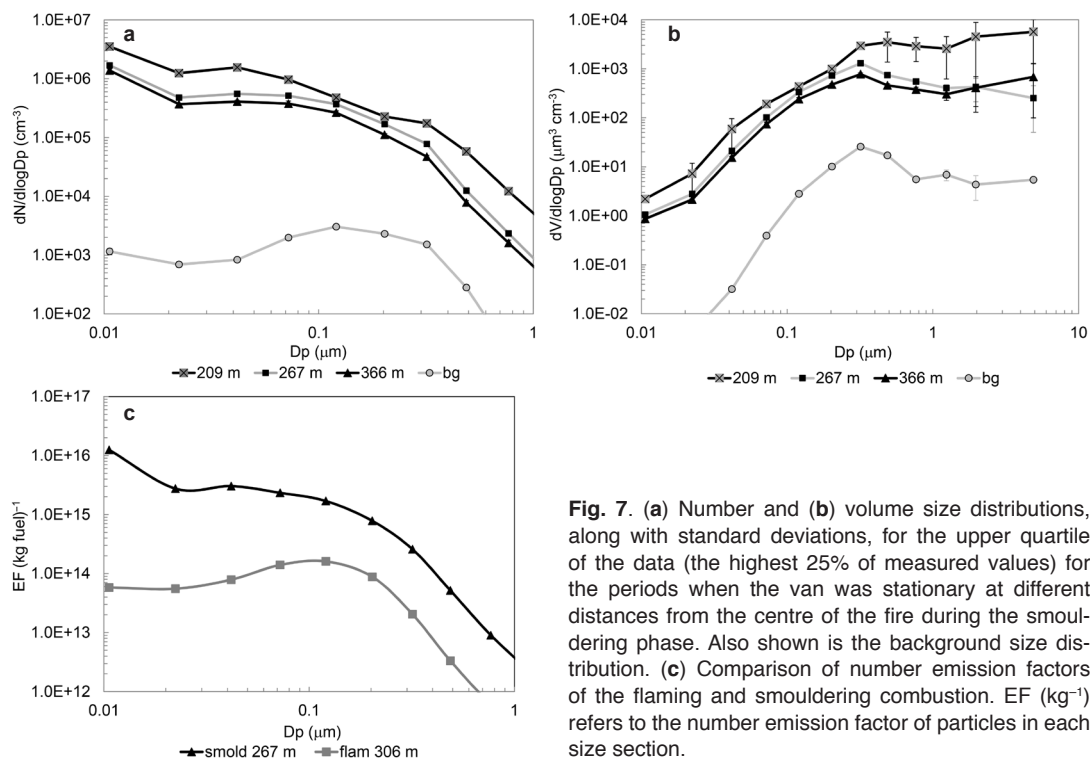| Flaming phase	N_{nuc} (cm^{-3} × 10^4)	D_g (nm)	σ	N_{acc} (cm^{-3} × 10^4)	D_g (nm)	σ			
179 m	66.9	12.7	1.4	13.1	89.3	2.0			
194 m	2.7	14.4	1.8	6.5	96.9	1.9			
306 m	0.6	16.2	1.8	2.2	101.1	1.8			
1484 m	0.03	12.4	1.7	0.7	49.3	1.8			
1634 m	0.2	16.0	1.8	0.4	90.0	1.7			
Smouldering phase	N_{nuc} (cm^{-3} × 10^5)	D_g (nm)	σ	N_{Ait} (cm^{-3} × 10^5)	D_g (nm)	σ	N_{acc} (cm^{-3} × 10^5)	D_g (nm)	σ
209 m	33.7	6.1	1.7	10.7	41.9	1.9	0.98	263	2.0
267 m	8.8	9.5	1.6	4.3	69.6	2.0	0.04	458	1.8
366 m	10.5	7.3	1.8	3.4	63.8	2.0	0.05	400	1.9

Fig. 7. (**a**) Number and (**b**) volume size distributions, along with standard deviations, for the upper quartile of the data (the highest 25% of measured values) for the periods when the van was stationary at different distances from the centre of the fire during the smouldering phase. Also shown is the background size distribution. (**c**) Comparison of number emission factors of the flaming and smouldering combustion. EF (kg^{-1}) refers to the number emission factor of particles in each size section.

Due to the instrument limitation they could not measure nucleation mode particles. Petzold *et al.* (2007) measured aged forest fire particles with the modal diameters of 65–90 nm for the Aitken mode, 260–300 nm for accumulation mode, and 0.6–0.9 μm for the coarse modes. Reid *et al.* (2005) reported in the review paper the count median diameter of around 130 nm and the volume median diameter between 250–309 nm for the fresh boreal forest smoke. Janhäll *et al.* (2010) concluded that particles emitted during flaming combustion are commonly larger than those emitted during smouldering combustion.

Emission parameters

Linear regression analysis was used to determine the dependencies between peak excess concentrations of N_{tot}, PM$_{2.5}$, NO$_x$ and CO, and the excess CO$_2$ concentration (Fig. 8). Due to the limited amount of the data, the smouldering and flaming phases were not separated. Since $r^2 \geq 0.5$ for all studied species (Fig. 8), burning can be

considered the main source of these concentrations, as pointed out by Sinha *et al.* (2003).

The estimated emission factors are given in Table 3. The EF$_{CO}$ $\approx$ 52 g kg^{-1} is significantly smaller than found in other studies; for example: 118 g kg^{-1} from a prescribed burn with woody fuels (primarily Douglas fir) (Hobbs *et al.* 1996), 65 ± 20 g kg^{-1} for savanna/grassland and 104 ± 20 g kg^{-1} for tropical forest (Andreae and Merlet 2001), 135 ± 11 g kg^{-1} for conifer forest (Urbanski *et al.* 2013), and 127 g kg^{-1} for boreal forest (Burling *et al.* 2011). Different fuel used in this work and slow response time (> 30 s) of the CO analyser might explain this deviation. EF$_{NOx}$ is in good agreement with the results of the other studies in which EF$_{NOx}$ varied in the range of 1.6–3.9 g kg^{-1} (Andreae and Merlet 2001, Sinha *et al.* 2003, Yokelson *et al.* 2007, Burling *et al.* 2011).

As regards EF$_{Ntot}$, the results strongly depend on the size range detected by the instruments used, and only a few relevant studies were found in the literature. Guyon *et al.* (2005) estimated the emission factor of (0.5–2) × 10^{15} kg^{-1} for

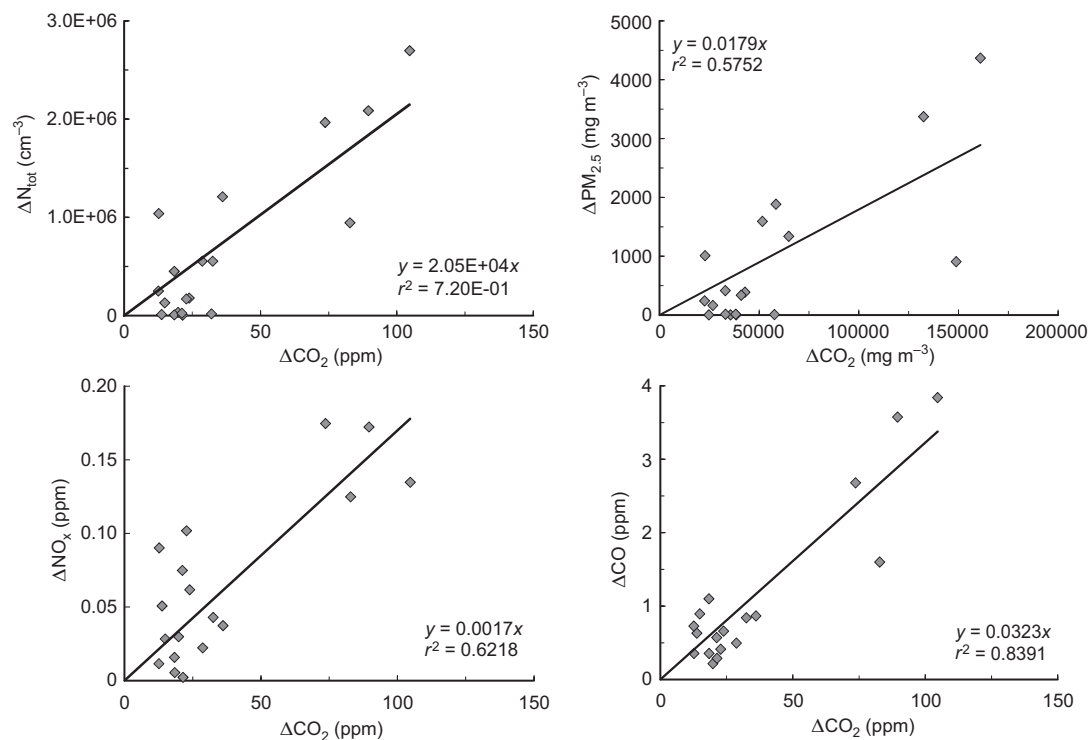**Fig. 8**. Dependence of excess (**a**) N_{tot}, (**b**) $PM_{2.5}$, (**c**) NO_x, and (**d**) CO on excess of CO_2.

particles in the size range of 8–300 nm from the tropical forest fire, and Sinha *et al*. (2003) clearly higher values $(30 \pm 17) \times 10^{15}$ kg^{-1} for particles larger than 3 nm from the savanna fire. Our value 18.4×10^{15} kg^{-1} is in an agreement with both. Virkkula *et al*. (2014a) estimated a lower value of 4.8×10^{15} kg^{-1} for EF$_{Ntot}$ during the flaming phase in the airborne measurements. Reid *et al*. (2005) reported a value of 20 ± 7.5 g (kg fuel)$^{-1}$ for the emission factor of $PM_{2.5}$ from the boreal forest fire, and Burling *et al*. (2011) somewhat higher value 24.2 g (kg fuel)$^{-1}$ from the prescribed boreal forest fire. Typically the amount of burned fuel per hectare is bigger on the prescribed burning compared to the wildfire. The result of this study, which was calculated from the peak values, is 29.0 g (kg fuel)$^{-1}$.

Table 3. Emission factors.

CO (g kg^{-1})	52.1 ± 3.7
NO$_x$ (g kg^{-1})	2.7 ± 0.3
N_{tot} (g kg^{-1})	$(18.4 \pm 2.0) \times 10^{15}$
PM$_{2.5}$ (kg^{-1})	29.0 ± 4.3

Summary and conclusions

This is the first study, in which ground-level concentrations and horizontal dispersion of the smoke plume from a fire were measured using a mobile laboratory. The measurements covered distances up to 1600 m from the burn area. During the flaming phase, only a minor fraction of the plume was detected at the ground level. The particle concentrations decreased as a function of distance from the burn area, due to dilution and also partly due to coagulation and other aerosol processes. Based on the simple function fitted to the measured particle number concentration data (Fig. 4), the smoke particle number concentration was around 25% of that at the burn area at a distance of 200 m, 5% at a distance of 1000 m, and approximately at the background level at a distance of 3500 m. Particle size distributions were dominated by the nucleation and accumulation modes. The particle size resolution and measurement cut-off size of the ELPI instrument posed limitations to the interpretation of the data. However, the lognormal fittings showed

an increase in modal diameters as a function of downwind distance, indicating that during dispersion the particles grew due to the condensation and coagulation processes.

During the smouldering phase, when dense smoke dispersed close to the ground surface, the particle number concentrations were around 10 times higher as compared with those during the flaming phase. Based on the 10-s data, the maximum concentration was 2.7×10^6 cm^{-3} in the plume at a distance of around 180 m from the centre of the burn area. Simultaneously, the CO_2 concentration was 104 ppm above the background level. The particle size distributions were dominated by small nucleation mode particles peaking at 6–10 nm, and Aitken mode particles peaking at 42–70 nm, even though some larger particles also existed.

Comparison of the emission factors of plume gases and particles with the corresponding previously published values is complicated due to several reasons. First, published values concern sometimes wild-land fires, sometimes prescribed fires, in some cases smouldering, and in some other cases flaming phases. Second, the fuel type differs depending on the forest or land-use type, and factors such as moisture of the burned material. Third, in case of particulate matter, there is wide range of cut-off sizes of particle number instruments used. Regardless of these complications, the estimated emission factors (in regard to the excess CO_2 concentrations) of this work for slash of the boreal forest are in good agreement with the previously published values. The only exception was CO, the emission factor of which was clearly lower than the published values, probably due to instrumental fault.

The obtained emission factor for the total particle number concentration per unit of mass burned EF_{Ntot} [$(18.4 \pm 2.0) \times 10^{15}$ kg^{-1}] was of the same order as the corresponding values for ship emissions, which typically are in the range of 5×10^{15}–1×10^{17} kg^{-1}. However, in case of fine particulate matter, $EF_{PM2.5}$ (29.0 ± 4.3 g kg^{-1}) was approximately one order of magnitude higher as compared with the corresponding values of ship emissions (e.g. Johnsson *et al.* 2011, Moldanova *et al.* 2013).

When conducting prescribed burning experiments in the future, we would recommend to use more mobile platforms, both ground-based and airborne. This would facilitate spatially and temporally pertinent measurements of the fire plumes even in situations, when atmospheric dispersion conditions, such as the wind direction, unexpectedly change. In our experiment, the "Sniffer" van proved to be a useful tool considering rapidly changing wind direction. It was obvious based both on visual observations (Virkkula *et al.* 2014b) and dispersion model computations (Kukkonen *et al.* 2014) that the most intensive smoke plumes from the fire did not reach the instrumentation on the SMEARII mast. The burning intensity also varied in time. Despite these difficulties, useful data were obtained both from the ground-based and airborne mobile measurements. The data from this work could also be used in the future for evaluating and refining of atmospheric models of buoyant plumes.

References

Akagi S.K., Yokelson R.J., Wiedinmyer C., Alvarado M.J., Reid J.S., Karl T., Crounse J.D. & Wennberg P.O. 2011. Emission factors for open and domestic biomass burning for use in atmospheric models. *Atmos. Chem. Phys.* 11: 4039–4072.

Andreae M.O. & Merlet P. 2001. Emissions of trace gases and aerosols from biomass burning. *Global Biogeochem. Cycl.* 15: 955–966.

Bond T.C., Doherty S.J., Fahey D.W., Forster P.M., Berntsen T., DeAngelo B.J., Flanner M.G., Ghan S., Kärcher B., Koch D., Kinne S., Kondeo Y., Quinn, P.K., Sarofim M.C:, Schultz M.G., Schulz M., Venkataraman C., Zhang H., Zhang S., Bellouin N., Guttikunda K., Hopke P.K., Jacobson M.Z., Kaiser J.W., Klimont Z., Lohmann U., Schwarz J.P., Shindell D., Storelvmo T., Warren S.G. & Zender C.S. 2013. Bounding the role of black carbon in the climate system: a scientific assessment. *J. Geophys. Res.* 118: 5318–5552.

Burling I.R., Yokelson R.J., Akagi S.K., Urbanski S.P., Wold C.E., Griffith D.W.T., Johnson T.J., Reardon J. & Weise D.R. 2011. Airborne and ground-based measurements

of the trace gases and particles emitted by prescribed fires in the United States. *Atmos. Chem. Phys.* 11: 12197–12216.

Carvalho A., Flanningan M.D., Logan K.A., Gowman L.M., Miranda A.I. & Borrego C. 2010. The impact of spatial resolution on area burned and fire occurrence projections in Portugal under climate change. *Climatic Change* 98: 177–197.

Charlson R.J., Schwartz S.E., Hales J.M., Cess R.D., Coakley J.A., Hansen J.E. & Hofmann D.J. 1992. Climate forcing by anthropogenic aerosols. *Science* 255: 423–430.

Crutzen P.J. & Andreae M.O. 1990. Biomass burning in the tropics: Impact on atmospheric chemistry and biogeochemical cycles. *Science* 50: 1669–1678.

Fiedler V., Arnold F., Ludmann S., Minikin A., Pirjola L., Dörnbrack A. & Schlager H. 2011. African biomass burning plumes over the Atlantic: aircraft based measurements and implications for H_2SO_4 and HNO_3 mediated smoke particle activation. *Atmos. Chem. Phys.* 11: 3211–3225.

Guyon P., Frank G.P., Welling P., Chand D., Artaxo P., Rizzo L., Nishioka G., Kolle O., Fritsch H., Silva Dias M.A.F., Gatti L.V., Gordova A.M. & Andreae M.O. 2005. Airborne measurements of trace gas and aerosol particle emissions from biomass burning in Amazonia. *Atmos. Chem. Phys.* 5: 2989–3002.

Hari P. & Kulmala M. 2005. Station for measuring ecosystem–atmosphere relations (SMEAR II). *Boreal Env. Res.* 10: 315–322.

Hobbs P.V., Reid J.S., Herring J.A., Nance J.D., Weiss R.E., Ross J.L., Hegg D.A., Ottmar R.D. & Liousse C. 1996. Particle and trace-gas measurements in smoke from prescribe ed burns of forest products in the Pacific Northwest. In: Levine J.S. (ed.), *Biomass burning and global change*, vol. 1, MIT Press, New York, pp. 697–715.

Hobbs P.V, Sinha P., Yokelson R.J., Christian T.J., Blake D.R., Goa S., Kirchstetter T.W., Novakov T. & Pilewskie P. 2003. Evolution of gases and particles from a savanna fire in South Africa. *J. Geophys. Res.* 108, D13, 8485, doi:10.1029/2002JD002352.

Hodzic A., Madronich S., Bohn B., Massie S., Menut L. & Wiedinmyer C. 2007. *Atmos. Chem. Phys.* 7: 4043–4046.

Janhäll S., Andreae, M.O. & Pöschl U. 2010. Biomass burning aerosol emissions from vegetation fires: particle number and mass emission factors and size distributions. *Atmos. Chem. Phys.* 10: 1427–1439.

Johnson Å.M., Westerlund J. & Hallquist M. 2011. Size-resolved particle emission factors for individual ships. *Geophys. Res. Lett.* 38, L13809, doi:13810.11029/12011GL047672.

Keskinen J., Pietarinen K. & Lehtimäki M. 1992. Electrical low pressure impactor. *J. Aerosol Sci.* 23: 353–360.

Kingham S., Durand M., Aberkane T., Harrison J., Wilson J.G. & Epton M. 2006. Winter comparison of TEOM, MiniVol and DustTrak PM10 monitors in a woodsmoke environment. *Atmos. Environ.* 40: 338–347.

Kukkonen J., Nikmo J., Sofiev M., Riikonen K., Petäjä T., Virkkula A., Levula J., Schobesberger S. & Webber D.M. 2014. Applicability of an integrated plume rise model for the dispersion from wild-land fires. *Geosci. Model Dev. Discuss.* 7: 483–527.

Klein T., Kukkonen J., Dahl Å., Bossioli E., Baklanov A., Vik A.F., Agnew P., Karatzas K.D. & Sofiev M. 2012. Interactions of physical, chemical, and biological weather calling for an integrated approach to assessment, forecasting, and communication of air quality. *Ambio* 41: 851–864.

Kumar P., Pirjola L., Ketzel M. & Harrison R.M. 2013. Nanoparticle emissions from 11 non-vehicle outdoor sources — a review. *Atmos. Environ.* 67: 252–277.

Marjamäki M., Ntziachristos L., Virtanen A., Ristimäki J., Keskinen J., Moisio M., Palonen M. & Lappi M. 2002. *Electrical filter stage for the ELPI*. Technical Paper 2002-01-0055, Society of Automotive Engineers (SAE).

Maruf Hossain A.M.M., Park S., Kim J.-S. & Park K. 2012. Volatility and mixing states of ultrafine particles from biomass burning. *J. Hazard. Mater.* 205–206: 189–197.

Moldanová J., Fridell E., Winnes H., Holmin-Fridell S., Boman J., Jedynska A., Tishkova V. & Demirdjian B. 2013. Physical and chemical characterisation of PM emissions from two ships operating in European Emission Control Areas. *Atmos. Meas. Tech.* 6: 3577–3596.

Morawska L., He C., Hitchins J., Mengersen K. & Gilbert D. 2003. Characteristics of particle number and mass concentrations in residential houses in Brisbane, Australia. *Atmos. Environ.* 37: 4195–4203.

Petzold A., Weinzierl B., Huntrieser H., Stolh A., Real E., Cozic J., Fiebig M., Hendricks J., Lauer A., Law K., Roiger A., Schlager H. & Weingartner E. 2007. Perturbation of the European free troposphere aerosol by North American forest fire plumes during the ICARTT-ITOP experiment in summer 2004. *Atmos. Chem. Phys.* 7: 5105–5127.

Pirjola L., Parviainen H., Hussein T., Valli A., Hämeri K., Aalto P., Virtanen A., Keskinen J., Pakkanen T., Mäkelä T. & Hillamo R. 2004. "Sniffer" — a novel tool for chasing vehicles and measuring traffic pollutants. *Atmos. Environ.* 38: 3625–3635.

Pirjola L., Paasonen P., Pfeiffer D., Hussein T., Hämeri K., Koskentalo T., Virtanen A., Rönkkö T., Keskinen J., Pakkanen T.A. & Hillamo R.E. 2006. Dispersion of particles and trace gases nearby a city highway: mobile laboratory measurements in Finland. *Atmos. Environ.* 40: 867–879.

Pirjola L., Lähde T., Niemi J.V., Kousa A., Rönkkö T., Karjalainen P., Keskinen J., Frey A. & Hillamo R. 2012. Spatial and temporal characterization of traffic emission in urban microenvironments with a mobile laboratory. *Atmos. Environ.* 63: 156–167.

Reid J.S., Koppmann R., Eck T.E. & Eleuterio D.P. 2005. A review of biomass burning emissions part II: intensive physical properties of biomass burning particles. *Atmos. Chem. Phys.* 5: 799–825.

Saarikoski S., Sillanpää M., Sofiev M., Timonen H., Saarnio K., Teinilä K., Karppinen A., Kukkonen J. & Hillamo R. 2007. Chemical composition of aerosols during a major biomass burning episode over northern Europe in spring 2006: Experimental and modelling assessments. *Atmos. Environ.* 41: 3577–3589.

Saarnio K., Aurela M., Timonen H., Saarikoski S., Teinilä K.,

Mäkelä T., Sofiev M., Koskinen J., Aalto P.P., Kulmala M., Kukkonen J. & Hillamo R. 2010. Chemical composition of fine particles in fresh smoke plumes from boreal forest-fires. *Sci. Total Environ.* 408: 2527–2542.

Seinfeld J.H. & Pandis S.N. 1998. *Atmospheric chemistry and physics: from air pollution to climate change*. John Wiley & Sons Inc., New York.

Simpson I.J., Akagi S.K., Barletta B., Blake N.J., Choi Y., Diskin G.S., Fried A., Fuelberg H.E., Meinardi S., Rowland F.S., Vay S.A., Weinheimer A.J., Wennberg P.O., Wiebring P., Wisthaler A., Yang M., Yokelson R.J. & Blake D.R. 2011. Boreal forest fire emissions in fresh Canadian smoke plumes: C_1–C_{10} volatile organic compounds (VOCs), CO_2, CO, NO_2, NO, HCN and CH_3CN. *Atmos. Chem. Phys.* 11: 6445–6463.

Sinha P., Hobbs P.V., Yokelson R.J., Bertschi I.T., Blake D.R., Simpson I.J., Gao S., Kirchstetter T.W. & Novakov T. 2003. Emissions of trace gases and particles from savanna fires in southern Africa. *J. Geophys. Res.* 108(D13), 8487, doi:10.1029/2002JD002325.

Sofiev M., Vankevich R., Lotjonen M., Prank M., Petukhov V., Ermakova T., Koskinen J. & Kukkonen J. 2009. An operational system for the assimilation of satellite information on wild-land fires for the needs of air quality modelling and forecasting, *Atmos. Chem. Phys.* 9: 6833–6847.

Urbanski S.P. 2013. Combustion efficiency and emission factors for wildfire-season fires in mixed conifer forests on the northern Rocky Mountains, US. *Atmos. Chem. Phys* 13: 7241–7262.

Ward D.E. & Hardy C.C. 1991. Smoke emission from wildland fires. *Environ. Int.* 17: 117–134.

Westerling A.L., Hidalgo H.G., Cayan D.R. & Swetnam T.W. 2006. Warming and earlier spring increase Western U.S. forest wildfire activity. *Science* 313: 940–943.

Virkkula A., Pohja T., Aalto P.P., Keronen P., Schobensberger S., Clements C.B., Petäjä T. & Kulmala M. 2014a. Airborne measurements of aerosols and corbon dioxide during a prescribed fire experiment at a boreal forest site. *Boreal Env. Res.* 19 (Suppl. B): 153–181.

Virkkula A., Levula J., Pohja T., Aalto P.P., Keronen P, Schobesberger S., Clements C.B., Pirjola L., Kieloaho A-J., Kulmala L., Aaltonen H., Patokoski J., Pumpanen J., Rinne J., Ruuskanen T., Pihlatie M., Manninen H.E., Aaltonen V., Junninen H., Petäjä T., Backman J., Dal Maso M., Nieminen T., Olsson T., Grönholm T., Aalto J., Virtanen T.H., Kajos M., Kerminen V.-M., Schultz D.M., Kukkonen J., Sofiev J., de Leeuw G., Bäck J., Hari P. & Kulmala M. 2014b. Prescribed burning of logging slash in the boreal forest in Finland: emissions and effects on meteorological quantities and soil properties. *Atmos. Chem. Phys.* 14: 1–30.

Yli-Ojanperä J., Kannosto J., Marjamäki M. & Keskinen J. 2010. Improving the nanoparticle resolution of the ELPI. *Aerosol and Air Quality Research* 10: 360–366.

Yokelson R.J., Karl T., Artaxo P., Blake D.R., Christian T.J., Griffith D.W.T., Guenther A. & Hao Q.M. 2007. The tropical forest and fire emissions experiment: overview and airborne fire emission factor measurements. *Atmos. Chem. Phys.* 7: 5175–5196.